Proc. Int. Conf. Heavy Electrons (ICHE2010)
J. Phys. Soc. Jpn. **80** (2011) SAonishi-iche2010

Multipole correlations of t_{2g}-orbital Hubbard model with spin-orbit coupling

Hiroaki Onishi*

Advanced Science Research Center, Japan Atomic Energy Agency, Tokai, Ibaraki 319-1195, JAPAN

We investigate the ground-state properties of a one-dimensional t_{2g}-orbital Hubbard model including an atomic spin-orbit coupling by using numerical methods, such as Lanczos diagonalization and density-matrix renormalization group. As the spin-orbit coupling increases, we find a ground-state transition from a paramegnetic state to a ferromagnetic state. In the ferromagnetic state, since the spin-orbit coupling mixes spin and orbital states with complex number coefficients, an antiferro-orbital state with complex orbitals appears. According to the appearance of the complex orbital state, we observe an enhancement of Γ_{4u} octupole correlations.

KEYWORDS: t_{2g} orbitals, spin-orbit coupling, multipole, density-matrix renormalization group

The competition and cooperation between spin and orbital degrees of freedom in strongly correlated electron systems manifest itself in the emergence of various types of spin-orbital ordered and quantum liquid phases.[1–3] In general, among competing interactions involving spin and orbital, the spin-orbit coupling is supposed to be weak in $3d$ transition-metal oxides such as cupurates and manganites, while as we move to $4d$ and $5d$ electrons, the spin-orbit coupling becomes strong and responsible for magnetic, transport, and optical properties. When the spin-orbit coupling is dominant, spin and orbital are not independent, but instead the total angular momentum gives a good description of the many-body state. In fact, it has been suggested that Sr_2IrO_4, in which Ir^{4+} ions have five electrons in triply degenerate t_{2g} orbitals, exhibits a novel Mott-insulating state with an effective total angular momentum $J_{\rm eff}$=1/2 due to a strong spin-orbit coupling.[4–7] In the limit of strong spin-orbit coupling, the ground-state Kramers doublet at a local ion can be described by an isospin with $J_{\rm eff}$=1/2.[8,9] The exchange interaction among isospins can lead to a variety of ordering and fluctuation phenomena of spin-orbital entangled states.

When we move to heavy-element f-electron systems such as rare-earth and actinide compounds, the spin-orbit coupling is large comparing with other energy scales. In such a case, we usually classify the complicated spin-orbital state from the viewpoint of multipole, which is described by the total angular momentum. Indeed, the multipole physics has been actively discussed in the field of heavy electrons.[10] A recent trend is to unveil exotic high-order multipole ordering. As an attempt to clarify multipole properties of f-electron systems from a microscopic viewpoint, we have numerically studied multipole correlations of an f-orbital Hubbard model on the basis of the j-j coupling scheme.[11] We believe that it is also important to clarify multipole properties in d-electron systems under the effect of the spin-orbit coupling.

In this paper, we investigate multipole properties in the ground state of a one-dimensional t_{2g}-orbital Hubbard model including the spin-orbit coupling by numerical methods. With increasing the spin-orbit coupling, the ground state changes from a paramagnetic state to a ferromagnetic state in terms of the magnitude of the total spin. In the ferromagnetic phase, antiferro-dipole correlations develop even when the spin state is ferromagnetic due to the orbital contribution. On the other hand, the spin-orbit coupling induces a complex orbital state, in which real xy, yz, and zx orbitals are mixed with complex number coefficients. According to the complex orbital state, Γ_{4u} octupole correlations are enhanced.

Let us consider triply degenerate t_{2g} orbitals on a one-dimensional chain along the x direction with five electrons per site. The one-dimensional t_{2g}-orbital Hubbard model with the spin-orbit coupling is described by

$$\begin{aligned} H =& \sum_{i,\tau,\tau',\sigma} t_{\tau\tau'}(d^{\dagger}_{i\tau\sigma}d_{i+1\tau'\sigma}+\mathrm{h.c.})+\lambda\sum_{i}\mathbf{L}_i\cdot\mathbf{S}_i \\ &+U\sum_{i,\tau}\rho_{i\tau\uparrow}\rho_{i\tau\downarrow}+(U'/2)\sum_{i,\sigma,\sigma',\tau\neq\tau'}\rho_{i\tau\sigma}\rho_{i\tau'\sigma'} \\ &+(J/2)\sum_{i,\sigma,\sigma',\tau\neq\tau'}d^{\dagger}_{i\tau\sigma}d^{\dagger}_{i\tau'\sigma'}d_{i\tau\sigma'}d_{i\tau'\sigma} \\ &+(J'/2)\sum_{i,\sigma\neq\sigma',\tau\neq\tau'}d^{\dagger}_{i\tau\sigma}d^{\dagger}_{i\tau\sigma'}d_{i\tau'\sigma'}d_{i\tau'\sigma}, \end{aligned} \qquad (1)$$

where $d_{i\tau\sigma}$ ($d^{\dagger}_{i\tau\sigma}$) is an annihilation (creation) operator for an electron with spin σ (=$\uparrow,\downarrow$) in orbital τ (=xy, yz, zx) at site i, and $\rho_{i\tau\sigma}$=$d^{\dagger}_{i\tau\sigma}d_{i\tau\sigma}$. The hopping amplitude is given by $t_{xy,xy}$=$t_{zx,zx}$=t and zero for other combinations of orbitals. Hereafter, t is taken as the energy unit. $\mathbf{L}_i$ and $\mathbf{S}_i$ represent orbital and spin angular momentum operators, respectively, and λ is the spin-orbit coupling. U, U', J, and J' denote intra-orbital Coulomb, inter-orbital Coulomb, exchange, and pair-hopping interactions, respectively. We assume U=U'+J+J' due to the rotation symmetry in the local orbital space and J'=J due to the reality of the orbital function.[12] Throughout this paper, we set $\hbar$=$k_{\rm B}$=1.

We investigate the ground-state properties of the model (1) by exploiting a finite-system density-matrix renormalization group (DMRG) method with open boundary conditions.[13] The number of states kept for each block is up to m=120, and the truncation error is estimated to be 10^{-4}∼10^{-5}. We remark that due to the three orbitals in one site, the number of bases for the single site is 64, and the size of the superblock

*E-mail address: onishi.hiroaki@jaea.go.jp

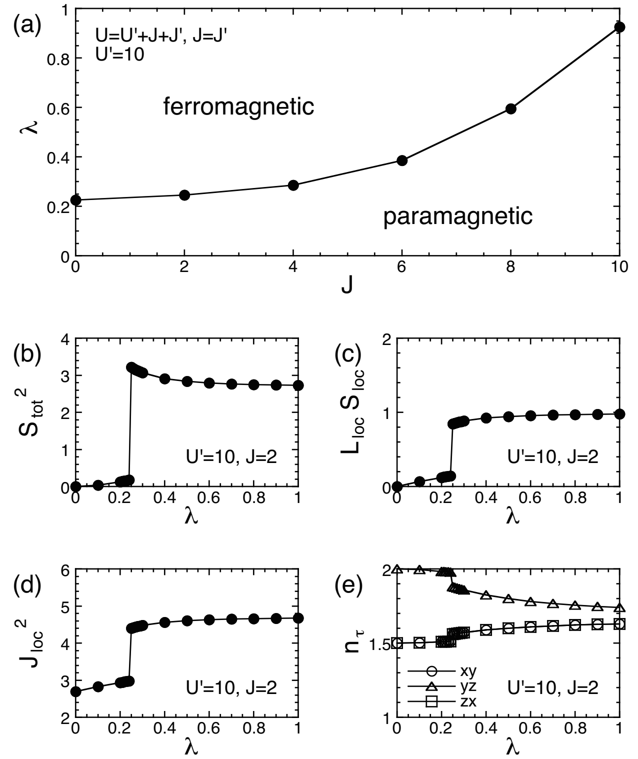

Fig. 1. Lanczos results for the four-site periodic chain. (a) The ground-state phase diagram in the (J,λ) plane for U'=10. (b) The magnitude of the total spin in the whole system. (c) The correlation between spin and orbital in the single site. (d) The magnitude of the total angular momentum in the single site. (e) The charge density in each orbital.

Hilbert space grows as $m^2\times 64^2$. To reduce the size of the Hilbert space, we usually decompose the Hilbert space into a block-diagonal form by using symmetries of the Hamiltonian. In the present case, however, the spin-orbit coupling breaks the spin SU(2) symmetry, so that we cannot utilize $S^z_{\rm tot}$ as a good quantum number, where $S^z_{\rm tot}$ is the z component of the total spin. Since we ignore $e_{\rm g}$ orbitals among d orbitals, the total angular momentum is not a conserved quantity. The total number of electrons can be used as a good quantum number. Thus, since DMRG calculations consume much CPU times, we supplementally use a Lanczos diagonalization method for the analysis of a four-site periodic chain to accumulate results with relatively short CPU times.

Let us first look at Lanczos results for the four-site periodic chain. In Fig. 1(a), we show the phase diagram in the (J,λ) plane for U'=10. The phase boundary is determined by the magnitude of the total spin $\mathbf{S}^2_{\rm tot}$. As shown in Fig. 1(b), $\mathbf{S}^2_{\rm tot}$ is almost zero for small λ, indicating a spin-singlet ground state. As λ increases, we find a transition to a ferromagnetic state with finite $\mathbf{S}^2_{\rm tot}$. Note that even in the limit of large λ, $\mathbf{S}^2_{\rm tot}$ does not approach the maximum value 2(2+1)=6, since the spin-orbit coupling mixes spin up and down states and the complete ferromagnetic state is disturbed. In Fig. 1(c), we plot the correlation between spin and orbital in the local site $\mathbf{L}_{\rm loc}\cdot\mathbf{S}_{\rm loc}$. At λ=0, there is no correlation between spin and orbital. As λ increases, the spin-orbital correlation develops and approaches one in the limit of large λ, indicating totally parallel spin and orbital angular momenta. In Fig. 1(d), the

Γ_γ multipole	multipole operator
Γ_{4u} dipole	J_x, J_y, J_z
Γ_{3g} quadrupole	O_u=(1/2)$(2J_z^2-J_x^2-J_y^2)$
	O_v=$(\sqrt{3}/2)(J_x^2-J_y^2)$
Γ_{5g} quadrupole	O_{yz}=$(\sqrt{3}/2)\overline{J_yJ_z}$
	O_{zx}=$(\sqrt{3}/2)\overline{J_zJ_x}$
	O_{xy}=$(\sqrt{3}/2)\overline{J_xJ_y}$
Γ_{2u} octupole	T_{xyz}=$(\sqrt{15}/6)\overline{J_xJ_yJ_z}$
Γ_{4u} octupole	T_x^α=(1/2)$(2J_x^3-\overline{J_xJ_y^2}-\overline{J_z^2J_x})$
	T_y^α=(1/2)$(2J_y^3-\overline{J_yJ_z^2}-\overline{J_x^2J_y})$
	T_z^α=(1/2)$(2J_z^3-\overline{J_zJ_x^2}-\overline{J_y^2J_z})$
Γ_{5u} octupole	T_x^β=$(\sqrt{15}/6)(\overline{J_xJ_y^2}-\overline{J_z^2J_x})$
	T_y^β=$(\sqrt{15}/6)(\overline{J_yJ_z^2}-\overline{J_x^2J_y})$
	T_z^β=$(\sqrt{15}/6)(\overline{J_zJ_x^2}-\overline{J_y^2J_z})$

Table I. Definition of multipole operators up to rank 3. The overline on the product denotes the operation of taking all possible permutations in terms of cartesian components, e.g., $\overline{J_xJ_y}$=J_xJ_y+J_yJ_x.

magnitude of the total angular momentum in the single site $\mathbf{J}^2_{\rm loc}$ is shown. At the transition point, $\mathbf{J}^2_{\rm loc}$ exhibits a sudden increase, since the spin-orbit coupling stabilizes a large total angular momentum state at every local sites. Note again that $\mathbf{J}^2_{\rm loc}$ does not reach the maximum value $\frac{5}{2}(\frac{5}{2}+1)$=$\frac{35}{4}$ in the limit of large λ, since the total angular momentum is not a conserved quantity. Regarding the orbital state, we show the charge density in each orbital in Fig. 1(e). Due to the spatial anisotropy of orbitals, one hole is preferably accommodated in itinerant xy or zx orbitals in each site, while localized yz orbitals are doubly occupied. Measuring charge correlations, we find that holes occupy real xy or zx orbital alternately for small λ (not shown). Namely, the ground state is a *real* orbital state. For large λ, however, xy, yz, and zx orbitals are mixed with complex number coefficients by the spin-orbit coupling, leading to a *complex* orbital state.

Now we move on to the analysis of multipole properties to clarify the ground-state properties from the viewpoint of multipole. We measure multipole correlation functions

$$\chi_{\Gamma_\gamma}(q)=\sum_{j,k}\langle X_{j\Gamma_\gamma}X_{k\Gamma_\gamma}\rangle {\rm e}^{{\rm i}q(j-k)}/N, \tag{2}$$

where $X_{i\Gamma_\gamma}$ is a multipole operator with the symbol X of multipole for the irreducible representation Γ_γ in the cubic symmetry at site i. Here, we consider 15 types of multipoles including three dipoles (X=J), five quadrupoles (X=O), and seven octupoles (X=T), as listed in Table I.[14] We evaluate the multipole correlation functions by DMRG calculations with chains of 16 sites.

Figure 2 shows DMRG results of the multipole correlation functions at U'=10, J=2, and λ=0 for the paramagnetic phase. Regarding dipoles, as shown in Fig. 2(a), the J_x correlation has a peak at q=π, which signals an antiferromagnetic state. Here, we notice that each of the dipole correlations exhibits a kink at q=$\pi/2$, while the kink corresponds to a peak for the J_y and J_z correlations. This kink structure originates in the spin-orbital SU(4) symmetry which realizes at a special point J=λ=0.[15–19] At the SU(4) symmetric point, correlations of spin $\mathbf{S}_i$ and orbital pseudospin $\mathbf{T}_i$=$\frac{1}{2}\sum_{\tau,\tau',\sigma}d^\dagger_{i\tau\sigma}\boldsymbol{\sigma}_{\tau\tau'}d_{i\tau'\sigma}$, where $\boldsymbol{\sigma}$ are Pauli matrices, coincide with each other and have a peak at q=$\pi/2$. With increasing J, the spin correlation of q=$\pi/2$ grows and the peak of the spin correlation remains at

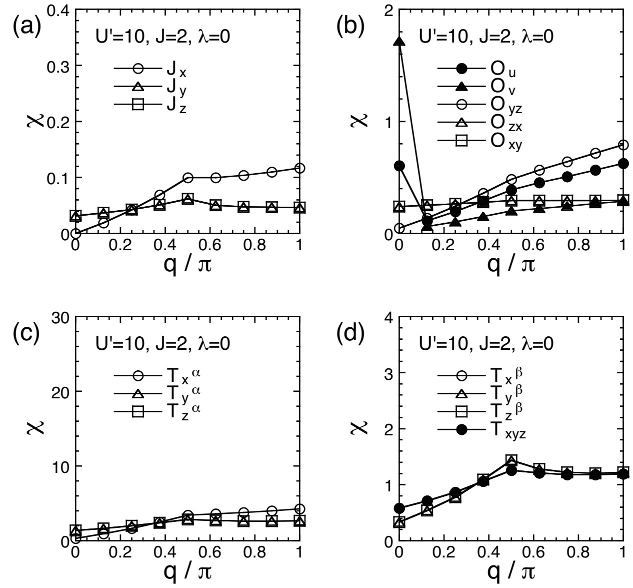

Fig. 2. DMRG results of multipole correlations at U'=10, J=2, and λ=0: (a) Γ_{4u} dipoles; (b) Γ_{3g} and Γ_{5g} quadrupoles; (c) Γ_{4u} octupoles; and (d) Γ_{5u} and Γ_{2u} octupoles.

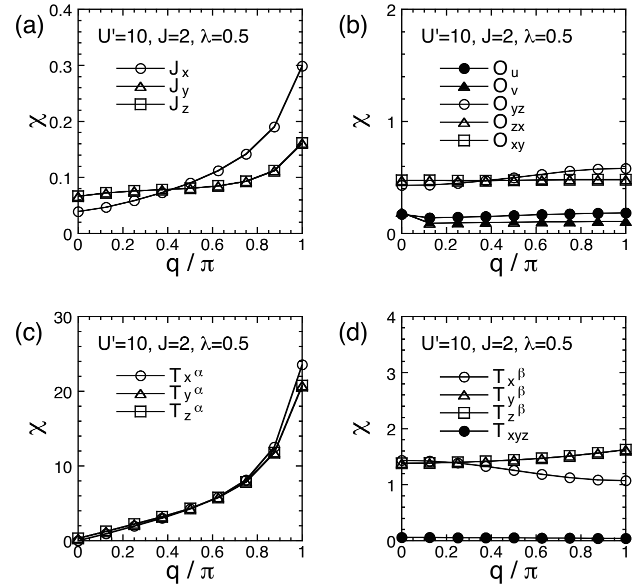

Fig. 3. DMRG results of multipole correlations at U'=10, J=2, and λ=0.5: (a) Γ_{4u} dipoles; (b) Γ_{3g} and Γ_{5g} quadrupoles; (c) Γ_{4u} octupoles; and (d) Γ_{5u} and Γ_{2u} octupoles.

q=$\pi/2$. On the other hand, the pseudospin correlation of q=π is enhanced, and the peak position of the pseudospin correlation changes to q=π. Note that for the orbital angular momentum $\mathbf{L}_i$, the correlation of the q=π component is enhanced as well. Thus, the orbital contribution to dipole leads to the peak of the J_x correlation at q=π rather than q=$\pi/2$.

In Fig. 2(b), we find that for the O_u and O_v correlations, a sharp peak appears at q=0, since $\langle O_u \rangle$ and $\langle O_v \rangle$ are turned out to be finite. We also find a peak at q=π for the O_u, O_v, and O_{yz} correlations, implying an antiferro-orbital state. For all quadrupoles, there occurs a kink at q=$\pi/2$ in similar to the case of dipoles, which is a trace of the SU(4) symmetry at J=λ=0. As shown in Fig. 2(c) and 2(d), we also observe a kink at q=$\pi/2$ for octupoles.

In Fig. 3, we present the multipole correlation functions at U'=10, J=2, and λ=0.5 for the ferromagnetic phase. At a glance, we find that the kink structure at q=$\pi/2$ disappears for all multipoles. Concerning dipoles, as shown in Fig. 3(a), a peak appears at q=π. Namely, antiferro-dipole correlations become dominant even when the spin state is ferromagnetic due to the orbital contribution. In fact, the spin $\mathbf{S}_i$ correlation has a peak at q=0, while the orbital $\mathbf{L}_i$ correlation exhibits a peak at q=π (not shown). On the other hand, the quadrupole correlations are found to be almost flat, and we cannot see any fine structures signaling quadrupole ordering, as shown in Fig. 3(b). As for octupoles, we observe a significant enhancement of the Γ_{4u} octupole correlations of the q=π component [see Figs. 2(c) and 3(c)]. The growth of the antiferro-octupole correlations reflects the stabilization of the antiferro-orbital state with complex orbitals.

In summary, we have studied the ground-state properites of the t_{2g}-orbital Hubbard model with the spin-orbit coupling from the viewpoint of multipole, by numerical techniques. The strong spin-orbit coupling induces a transition from the antiferromagnetic state to the ferromagnetic state. We have found that antiferro-dipole correlations develop even when the spin state is ferromagnetic. Moreover, the complex orbital state appears, since the spin-orbit coupling yields the linear combinations of spin and orbital states with complex number coefficients. Accordingly, we observe an enhancement of the Γ_{4u} octupole correlations. It is an interesting issue to explore possible multipole ordering in $5d$-electron Ir compounds with strong spin-orbit coupling.

The author thanks G. Khaliullin, S. Maekawa, and M. Mori for useful discussions. This work was supported by Grant-in-Aid for Scientific Research of Ministry of Education, Culture, Sports, Science, and Technoloty of Japan.

1) *Proc. Int. Conf. Strongly Correlated Electrons with Orbital Degrees of Freedom (ORBITAL2001)*, J. Phys. Soc. Jpn. **71** (2002) Suppl.
2) Y. Tokura and N. Nagaosa: Science **288** (2000) 462.
3) T. Hotta: Rep. Prog. Phys. **69** (2006) 2061.
4) B. J. Kim, H. Jin, S. J. Moon, J.-Y. Kim, B.-G. Park, C. S. Leem, J. Yu, T. W. Noh, C. Kim, S.-J. Oh, J.-H. Park, V. Durairaj, G. Cao, and E. Rotenberg: Phys. Rev. Lett. **101** (2008) 076402.
5) B. J. Kim, H. Ohsumi, T. Komesu, S. Sakai, T. Morita, H. Takagi, and T. Arima: Science **323** (2009) 1329.
6) S. Chikara, O. Korneta, W. P. Crummett, L. E. DeLong, P. Schlottmann, and G. Cao: Phys. Rev. B **80** (2009) 140407.
7) S. J. Moon, H. Jin, W. S. Choi, J. S. Lee, S. S. A. Seo, J. Yu, G. Cao, T. W. Noh, and Y. S. Lee: Phys. Rev. B **80** (2009) 195110.
8) H. Jin, H. Jeong, T. Ozaki, and J. Yu: Phys. Rev. B **80** (2009) 075112.
9) G. Jackeli and G. Khaliullin: Phys. Rev. Lett. **102** (2009) 017205.
10) Y. Kuramoto, H. Kusunose, and A. Kiss: J. Phys. Soc. Jpn. **78** (2009) 072001.
11) H. Onishi and T. Hotta: J. Phys. Soc. Jpn. **75** Suppl. (2006) 266.
12) E. Dagotto, T. Hotta, and A. Moreo: Phys. Rep. **344** (2001) 1.
13) S. R. White: Phys. Rev. Lett. **93** (1992) 2863.
14) R. Shiina, H. Shiba, and P. Thalmeier: J. Phys. Soc. Jpn. **66** (1997) 1741.
15) Y. Yamashita, N. Shibata, and K. Ueda: Phys. Rev. B **58** (1998) 9114.
16) H. C. Lee, P. Azaria, and E. Boulat: Phys. Rev. B **69** (2004) 155109.
17) J. C. Xavier, H. Onishi, T. Hotta, and E. Dagotto: Phys. Rev. B **73** (2006) 014405.
18) H. Onishi and T. Hotta: J. Magn. Magn. Mater. **310** (2007) 790.
19) H. Onishi: Phys. Rev. B **76** (2007) 014441.